IEEE Access
Multidisciplinary ⋮ Rapid Review ⋮ Open Access Journal

Received 12 April 2025, accepted 29 June 2025, date of publication 4 July 2025, date of current version 10 July 2025.

Digital Object Identifier 10.1109/ACCESS.2025.3585952

RESEARCH ARTICLE

Comparative Analysis of Machine Learning Algorithms for Antenna Alignments

MOHAMMAD AL BATAINEH, DANA I. ABU ABDOUN, AND MAHMOUD AL AHMAD, (Senior Member, IEEE)
Department of Electrical and Communication Engineering, United Arab Emirates University, Al Ain, United Arab Emirates
Corresponding author: Mohammad Al Bataineh (mffbataineh@uaeu.ac.ae)

This work was supported in part by the United Arab Emirates University Research Office. The Article Processing Charge (APC) was paid by the Research and Sponsored Projects Office at UAEU.

ABSTRACT In the rapidly evolving field of radio frequency (RF) engineering, precise antenna alignment remains a critical challenge, directly influencing communication performance and reliability. This study presents a comprehensive comparative analysis of three advanced machine learning models—Long Short-Term Memory (LSTM), Convolutional Neural Network (CNN), and Multilayer Perceptron (MLP)—to predict antenna alignments based on S-parameter measurements. By addressing the complexities of both distance and angle predictions, our approach demonstrates the efficacy of these neural network architectures in automating alignment tasks traditionally reliant on manual intervention. The results reveal that the MLP and LSTM models excel in distance prediction, achieving a remarkable accuracy of 97%, while the CNN model outperforms in angle prediction with an accuracy of 86%. This is the first work to propose a data-driven antenna alignment method based solely on S-parameter analysis, offering a cost-effective and scalable alternative to complex imaging or optical systems. The approach significantly reduces setup complexity while maintaining high prediction accuracy, making it well-suited for deployment in practical RF systems. The study further highlights the strengths and limitations of each model, offering valuable insights into their applicability for RF engineering tasks. By providing a robust machine learning framework, this research contributes significantly to advancing automated alignment processes, reducing dependency on manual methods, and paving the way for future innovations in RF systems. These findings have far-reaching implications for the development of intelligent and scalable solutions in wireless communication systems.

INDEX TERMS Antenna alignment, decision tree, machine learning algorithms, multilayer perceptron (MLP), random forest, RF engineering, S-parameters.

I. INTRODUCTION

In electromagnetic wave metrology, the evaluation of antenna characteristics is a fundamental measurement criterion. These characteristics, including power gain, energy distribution, radiation patterns, and polarization properties [1], [2], are essential to the operational integrity of high-frequency transmission systems. Therefore, the prompt identification, elucidation, and categorization of S-parameters are imperative to ensure the optimal performance of these systems.

S-parameters have been extensively employed in various analytical endeavors within the literature, encompassing applications such as frequency identification [3], analysis of radiation patterns, examination of power transmission characteristics, cable length prediction [4], and analyses of multiple input, multiple output antenna arrays [5]. This study proposes a novel application of S-parameters, specifically their utilization for antenna alignment. Traditionally, mechanical alignment tasks in assembly or measurement relied heavily on manual execution, demanding high skill levels but often resulting in low consistency and accuracy. Technological advancements have shifted this paradigm towards automation to meet growing demands for precision and volume. This shift has been facilitated through various technologies such as ultrasonic [6], [7], infrared [7], optical [8], [9], and imaging techniques.

The associate editor coordinating the review of this manuscript and approving it for publication was Tanweer Ali.

Previous approaches to alignment have demonstrated innovative yet often complex and costly methods. For instance, the alignment of a robotic arm [10] has been achieved using industrial cameras mounted on the arm's end, enabling alignment through image acquisition and feature extraction, although this adds significant cost and space requirements. Another approach utilized optical transmission measurements [11], demonstrating alignment for layer-by-layer assembly by measuring the spectral intensity of light transmitted through light-blocking optical alignment rulers (LBOARs) attached to the aligned wafer layers. Despite the small size of LBOARs (0.04 mm^2 for aligning two chips), they necessitate complex design and precision manufacturing. Furthermore, the non-contact alignment method using acoustic radiative forces [12], generated by ultrasound transducer arrays for aligning lightweight balloons, although innovative, requires visual feedback and is limited by the weight of the load.

In recent years, radio frequency (RF) engineering has increasingly intersected with machine learning, as machine learning techniques have proven effective in tackling complex signal processing tasks that traditional methods struggle to handle [13], [14]. With advancements in areas like 5G and IoT, the demand for highly precise, automated RF systems is greater than ever [15]. However, RF systems often encounter challenges like noise and interference, which can affect signal quality and reliability in practical applications [16]. Machine learning algorithms, especially deep learning, are being applied to tasks such as modulation recognition [13], spectrum management [17], and signal classification [14], transforming RF system capabilities. Furthermore, data-driven approaches are showing potential in automating RF design and simulation processes, making systems more efficient and adaptive [18], [19]. Despite these advances, there remains a gap in applying machine learning specifically for antenna alignment in RF systems, particularly for applications that require precise adjustments in both orientation and spacing.

While various alignment methods have emerged, few studies have directly explored the potential of RF antennas specifically for alignment purposes. Most research in this area has focused on methods involving radar [20] or radio-frequency identification (RFID) [21] principles, which traditionally do not account for object orientation. While some RFID-based systems have attempted to detect orientation through antenna polarization [22], these systems typically yield only binary alignment outcomes, limiting their utility in applications requiring precise orientation and spacing adjustments. Thus, there remains a critical need for cost-effective, high-precision alignment methods in RF engineering, particularly approaches that offer finer granularity in predicting both distance and angle alignments.

This study addresses this gap by introducing a novel, machine-learning-based approach to RF alignment that leverages S-parameter measurements. Specifically, we explore the potential of machine learning algorithms—Multilayer Perceptron (MLP), Convolutional Neural Network (CNN), and Long Short-Term Memory (LSTM)—to predict alignment with high accuracy and efficiency, focusing on both gap and angular misalignments using only S-parameter data. This approach diverges from traditional alignment methods by utilizing advanced data-driven models to handle complex RF alignment scenarios, providing a scalable, user-friendly solution. By evaluating and comparing these models, this study demonstrates the potential of machine learning to significantly improve alignment precision and process efficiency in RF systems.

TABLE 1. Comparison with reported works.

Ref.	Method	Assembly	Operation	Orientation detection
[10]	Imaging	Complex	Simple	Yes
[11]	Optical	Complex	Simple	Yes
[12]	Acoustic	Complex	Complex	Yes
[20]	RF - Radar	Complex	Simple	No
[21]	RF - RFID	Medium	Complex	No
[22]	RF - RFID	Medium	Medium	Yes
This Work	**RF - Antenna**	**Simple**	**Simple**	**Yes**

Compared to the studies outlined in Table 1, our approach presents a cost-effective and practical alternative to methods that rely on complex or costly instrumentation, such as optical, acoustic, or radar-based systems. Through its novel application of machine learning, this study establishes a foundational framework for future RF alignment applications, offering insights that could enhance wireless communication and other fields requiring precise component positioning.

This work pioneers the use of machine learning techniques—namely MLP, CNN, and LSTM—for antenna alignment prediction using S-parameter measurements, an approach not previously explored in existing literature. By training these models on a novel dataset composed of reflection and transmission coefficients, the proposed framework achieves a remarkable 97% accuracy in distance prediction using MLP and LSTM, and 86% accuracy in angle prediction using CNN. Unlike traditional methods that rely on expensive and complex setups involving cameras, optical systems, or acoustic arrays, our approach offers a cost-effective, accurate, and scalable solution that only requires standard S-parameter measurements. This paradigm shift toward data-driven alignment significantly simplifies implementation while preserving high precision, thereby enabling more intelligent and automated RF systems.

The rest of the paper is organized as follows: Section II provides an overview of the theoretical background crucial to this research, covering S-parameters and the principles of gap and angular alignment in antenna configurations. Section III details the methodology, including dataset preparation and the selection criteria for machine learning algorithms. Section IV presents the comparative analysis of algorithm performances, highlighting accuracy and predictive capabilities, and discusses these results. Finally, Section V concludes with a summary of findings and suggestions for future research.

II. THEORETICAL BACKGROUND

This section provides the theoretical background essential for understanding the methodologies and analysis conducted in this work.

A. S-PARAMETERS IN ANTENNA MEASUREMENT AND ANALYSIS

S-parameters, or scattering parameters, are fundamental metrics used to describe the electrical behavior of linear electrical networks when undergoing various signal interactions. They serve as a crucial tool in the analysis and design of RF and microwave circuits, providing insight into how signals are reflected and transmitted through a network. Specifically, S-parameters measure a network's complex reflection using coefficients (denoted as S_{11} and S_{22} for input and output ports, respectively) and complex transmission using transmission coefficients (S_{12} and S_{21} for forward and reverse transmission, respectively). In general, S_{NM} typically denotes the energy transferred from Port M to Port N [23]. These parameters are essential for understanding the performance characteristics of antennas and circuits, such as their impedance matching, signal loss, and the phase shift of signals passing through the network. The S-parameter analysis enables engineers to optimize the design and performance of RF components, ensuring their efficient operation within communication systems, thereby bridging the gap between theoretical design considerations and practical application outcomes.

B. ANTENNA GAP AND ANGULAR ADJUSTMENT

The two aspects of alignment can be categorized into *gap alignment* and *angular alignment*. This can be explained by considering two identical objects facing each other in the z-direction with their axes aligned. Gap alignment refers to adjusting the separation between two objects (Δz), while angular alignment refers to the angular displacement between them ($\Delta\phi$). The transmission coefficients can be used for gap alignment [24], [25], and the reflection coefficients can be used for angular and offset alignment [26], [27]. This is discussed subsequently.

Consider gap alignment, which can be adjusted using measurements of the transmission coefficient. At very short distances, the antennas operate in the near field. The well-known Friis equation governs link propagation in the far field. However, it has been modified for the near-field, depending on whether the transmission is between like sources (both are electric or both magnetic) or unlike sources (one electric and the other magnetic). In this case, the antennas are like magnetic sources with the same gain. Therefore, the link law becomes [28]:

$$\frac{P_R}{P_T} = \frac{G^2}{4}\left(\frac{1}{(k\Delta z)^2} - \frac{1}{(k\Delta z)^4} + \frac{1}{(k\Delta z)^6}\right), \qquad (1)$$

where $k = \frac{2\pi f}{c}$, Δz is the antenna spacing or gap alignment, G^2 is the product of the antenna gains, and P_R and P_T are the received and transmitted powers, respectively.

III. METHODOLOGY

This section presents the experimental setup and modeling pipeline for the proposed novel use of S-parameter-based machine learning models for antenna alignment.

The methodology underpinning our study involves a comprehensive approach, starting from the experimental setup to the application of machine learning models for predicting the mechanical alignment of antennas. This section outlines the sequential steps taken in our research, ensuring a systematic exploration of the predictive capabilities of various models.

Our experimental configuration, detailed in Figure 1(a), illustrates the physical arrangement of two identical antennas and their connection to a Rohde & Schwarz R&S® ZVL vector network analyzer (VNA) [29] via coaxial cable. The antennas are LTCC-based, with dimensions of 37 mm × 24 mm, a bandwidth of 25 MHz, and a resonant frequency of 2.32 GHz. Their reflection and transmission coefficients were measured under different alignment configurations. The VNA has a frequency range of 9 kHz to 13.6 GHz, a dynamic range of 85 dB to 105 dB, and a resolution of less than 0.5 dB for transmission measurements and less than 3 dB for reflection measurements. Prior to the measurements, the VNA was calibrated to ensure accurate results.

In the conducted experiments for gap alignment, the separation distance between the two antennas, denoted as Δz, was adjusted to several distinct values (0 mm, 2 mm, 13 mm, and 150 mm), with subsequent measurements of both reflection (S_{11} and S_{22}) and transmission (S_{21} and S_{12}) coefficients at each specified distance. For the angular alignment investigations, the gap Δz was maintained at zero. The setup involved securely fixing one antenna, as depicted in Figure 1(b), while the other was precisely rotated around its feed point in 30° increments, utilizing the ϕ axis of the antenna measurement tripod, as illustrated in Figure 1(c). Measurements of the reflection and transmission coefficients were systematically recorded for each angular position.

Our methodology, depicted in Figure 2, outlines a structured approach to predicting the mechanical alignment of antennas using machine learning models. This visual guide encompasses the entire experimental and analytical process, from the initial data collection to the final analysis of results.

A. DATASET DESCRIPTION

The dataset used in this study consists of a structured collection of S-parameter measurements derived from uniformly designed RF antennas. It includes a diverse range of mechanical alignments, focusing on two critical variables: the inter-antenna distance and the angular orientation. The dataset is fundamentally characterized by S_{11} and S_{22} parameters, which correspond to reflection coefficients, and S_{21} and S_{12} parameters, which correspond to transmission coefficients. These parameters are recorded over a refined

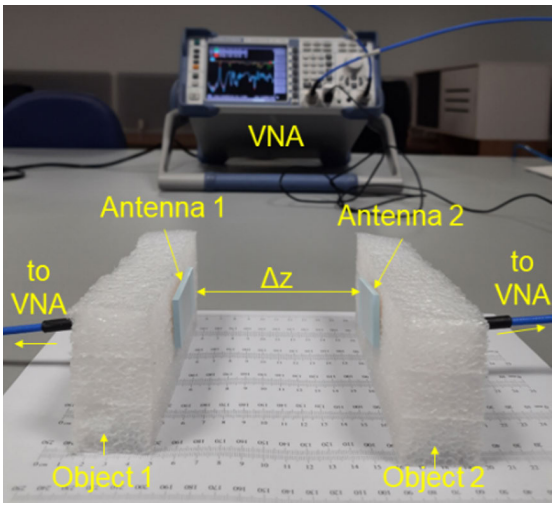

(a)

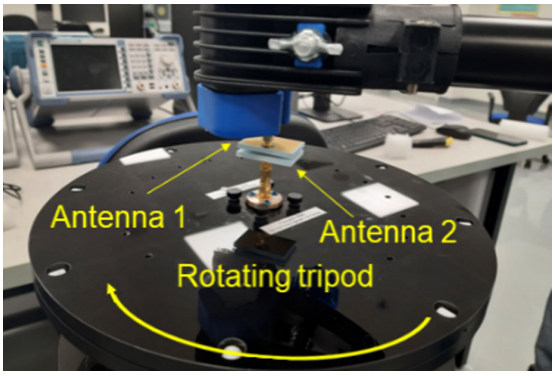

(b)

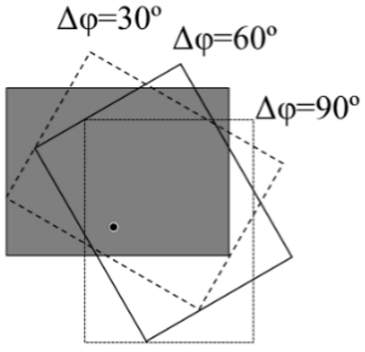

(c)

FIGURE 1. Experimental setup for (a) gap alignment measurements, (b) angular alignment, and (c) antenna alignment showing specific values of $\Delta\phi = 30°$, 60°, and 90°.

frequency range of 1 GHz to 3.01 GHz, providing a focused and comprehensive analysis of antenna behavior in different alignment states. The dataset records gap distances of 0 mm, 2 mm, 13 mm, and 150 mm, with angular measurements spanning from 30° to a complete circular rotation in 30° increments.

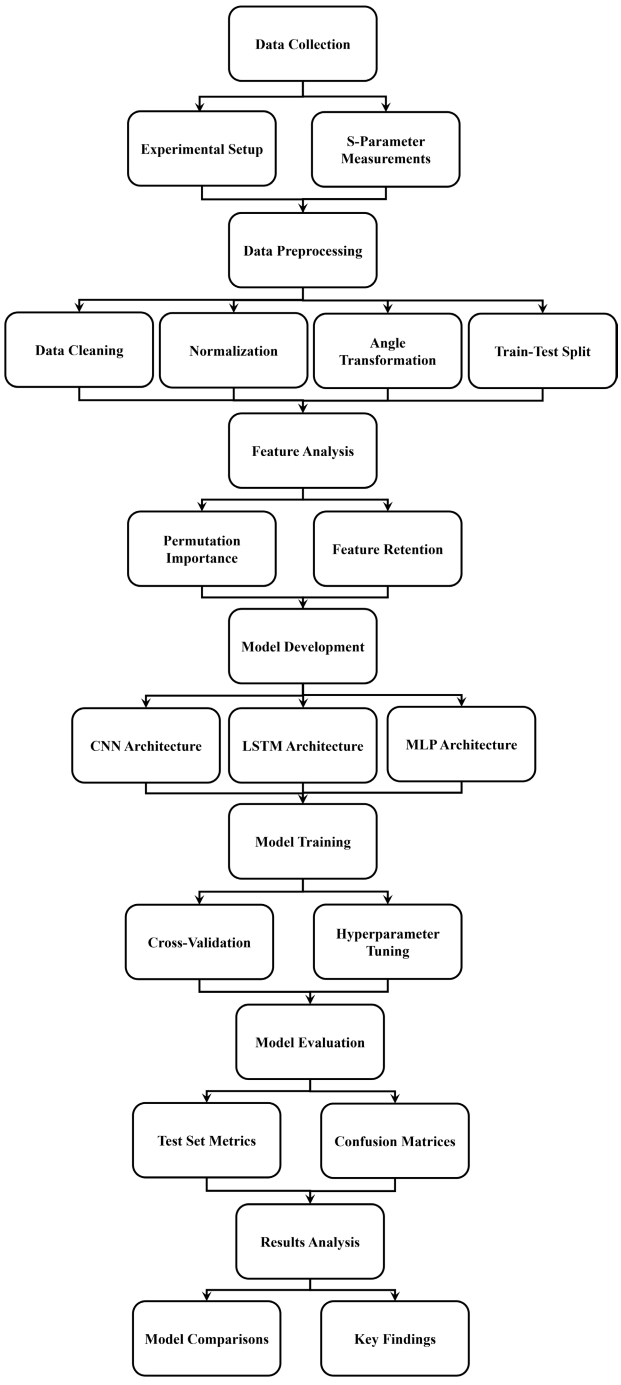

FIGURE 2. Methodological approach to machine learning-based prediction of antenna alignments.

The experimental setup, involving two identical antennas mounted on adjacent faces of two objects, facilitates direct S-parameter measurement across different alignment configurations without the need for conventional, more costly alignment methods. Compared to vision-based or optical alignment systems, this setup offers a low-cost, compact, and efficient alternative that relies solely on standard S-parameter measurements. This setup underscores the dataset's potential in providing a low-cost, effective solution for achieving

mechanical alignment, particularly focusing on gap alignment and angular displacement identification.

By integrating S-parameter measurements with the concept of electronic feedback and control circuits, the dataset emerges as a foundational tool for developing machine learning models that predict mechanical alignments with high precision. It represents the intersection of antenna technology and advanced analytics, paving the way for innovative approaches to optimize frequency transmission performance through accurate antenna alignment.

The statistical distribution of the dataset, summarized in Table 2, provides an in-depth overview of the collected measurements, reflecting the extensive operational bandwidth and the variability in alignment scenarios. The dataset consists of 4,001 instances, highlighting its comprehensive nature. The mean distance of 41.25 mm and standard deviation of 62.99 mm demonstrate a broad distribution of gap configurations, ranging from a minimum of 0 mm to a maximum of 150 mm. Similarly, angular measurements show a uniform distribution across the full circular range, with a mean of 180° and a standard deviation of 112.26°. The frequency values, spanning from 2 GHz to 3.01 GHz, reflect the dataset's focus on a critical operational bandwidth for RF antennas. Statistical summaries for S_{11}, S_{22}, S_{12}, and S_{21} reveal the expected variations in magnitude and phase, consistent with realistic antenna alignment conditions.

Figure 3 provides a refined depiction of the S-parameters measured at a spacing of 2 mm and an angular alignment of 0°. Figure 3(a) presents the magnitude responses of the four key S-parameters (S_{11}, S_{21}, S_{12}, and S_{22}) across a frequency range of 2.0 GHz to 2.6 GHz. The reflection coefficients (S_{11} and S_{22}) exhibit sharp notches near resonance, while the transmission coefficients (S_{21} and S_{12}) show strong peaks at approximately 2.32 GHz. The 10 dB bandwidth, calculated from the S_{21} response, is approximately 25 MHz, confirming the operating bandwidth of the antenna system as previously reported. This supports the antenna's suitability for applications requiring narrowband operation with high precision.

Figure 3(b) displays the phase characteristics of the same S-parameters. The phase transitions are especially pronounced around the resonant frequency, capturing the reactive dynamics and mutual coupling effects between ports. These phase and magnitude features provide essential indicators for training machine learning models to accurately classify alignment states based on S-parameter behavior under close-proximity conditions. To the best of our knowledge, this is the first dataset specifically designed to explore both gap and angular antenna alignment prediction using raw S-parameter measurements.

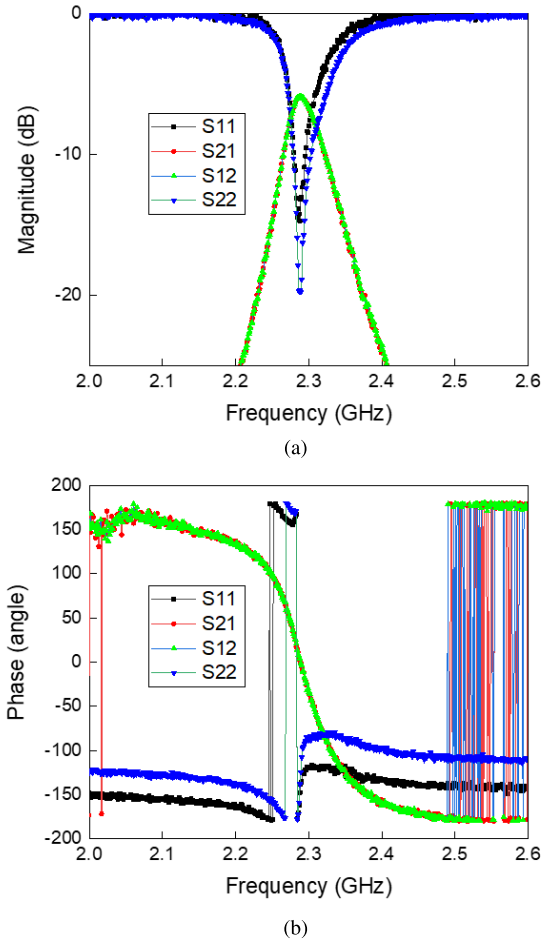

FIGURE 3. Analysis of S-parameters at 2 mm distance and 0°:(a) S_{11}, S_{21}, S_{12}, and S_{22} magnitude vs. frequency,(b) S_{11}, S_{21}, S_{12}, and S_{22} phase vs. frequency.

B. DATA PRE-PROCESSING

The basis of effective machine learning model development lies in meticulous data preparation. This study employed a structured pre-processing pipeline to optimize the S-parameter dataset for predictive modeling. The dataset, characterized by a wide frequency range and critical variables such as gap distance and angular orientation, underwent normalization and transformation processes to ensure consistency and enhance model performance.

To address the varied scale of frequency values, a normalization process was applied to the frequency measurements. Normalization mitigates the potential for skewed model performance and ensures that frequency features contribute uniformly during the learning process, a critical consideration given the sensitivity of models like neural networks to feature scaling. Recognizing the cyclical nature of angular measurements, a trigonometric transformation was adopted. Each angle was decomposed into sine and cosine components to preserve the continuity of angular data. This transformation enabled the models to accurately interpret angles, particularly at boundary transitions between 0° and 360°, where traditional representations might introduce discontinuities.

The pre-processed dataset was then split into training and testing subsets, allocating 80% of the data for training and 20% for testing. This division ensures that the models are trained on a substantial portion of the data while reserving

TABLE 2. Descriptive statistical summary of the antenna alignment dataset.

Metric	Dist. (mm)	Angle (°)	Freq. (GHz)	S_{11} Mag (dB)	S_{11} Phase (°)	S_{12} Mag (dB)	S_{12} Phase (°)	S_{21} Mag (dB)	S_{21} Phase (°)	S_{22} Mag (dB)	S_{22} Phase (°)
Min	0.00	0.00	1.00	-1.17	-179.91	-43.18	-179.96	-42.21	-180.00	-0.81	-179.99
25%	0.00	90.00	1.49	-0.64	-88.75	-28.31	-88.42	-28.43	-91.08	-0.24	-90.09
50%	2.00	180.00	1.97	-0.50	3.74	-24.88	-0.39	-25.03	0.62	-0.10	-0.39
75%	13.00	270.00	2.48	-0.36	92.82	-21.46	86.33	-21.67	85.18	0.04	86.29
Max	150.00	360.00	3.01	0.21	179.97	-2.60	179.86	-6.56	179.92	0.64	179.92
Mean	**41.07**	**182.90**	**2.01**	**-0.50**	**1.68**	**-24.88**	**-0.06**	**-25.01**	**-1.07**	**-0.10**	**-0.55**
Std. Dev.	**63.04**	**112.70**	**0.57**	**0.20**	**104.07**	**5.05**	**102.77**	**4.95**	**102.89**	**0.20**	**103.89**
Count	4001	4001	4001	4001	4001	4001	4001	4001	4001	4001	4001

a separate set for evaluating generalizability. The 80/20 split is a widely accepted standard that balances the need for robust model training with the ability to validate performance on unseen data. Splitting the data in this manner is particularly important for ensuring that the models are not overfitting to the training data, thereby improving their reliability in real-world applications.

Through these pre-processing steps, the dataset was transformed into a format suitable for machine learning models, ensuring that critical features and intrinsic data characteristics were preserved. This meticulous approach to data preparation underscores the importance of aligning pre-processing techniques with the unique properties of the dataset, enabling accurate and reliable predictions for both distance and angle classifications.

C. FEATURE SELECTION

To ensure that only the most informative features were used in predicting both distance and angle, a feature selection analysis was conducted. This was accomplished through an ablation study utilizing *permutation importance*, which assesses the impact of each feature on model performance by randomly shuffling feature values and observing the change in predictive accuracy.

Permutation importance was selected as it offers a straightforward, model-agnostic method to evaluate feature significance without relying on complex interactions or assumptions about data relationships. By measuring how each feature's randomization affected model accuracy, permutation importance provided a clear indication of each feature's contribution to the prediction task, allowing for an objective and interpretable evaluation.

Permutation importance values indicate how much model accuracy decreases when each feature is randomly shuffled. Higher values signify a stronger influence on prediction performance. In this study, scores above 2.0 suggest that a feature is highly influential and essential to model accuracy, scores between 1.0 and 2.0 indicate moderate influence, and scores below 0.5 imply minimal impact, suggesting limited relevance to the prediction task.

The results of the ablation study revealed distinct patterns in feature relevance for distance and angle predictions. For distance prediction, the transmission coefficient S_{21} showed the highest importance, with an average permutation importance score of 2.62, followed closely by S_{12} with a score of 2.52. These results underscore the significance of transmission coefficients in capturing distance-related information between antennas. Frequency also contributed meaningfully, with a permutation importance score of 1.11, though it was less influential than the transmission coefficients.

On the other hand, for angle prediction, the reflection coefficients S_{11} and S_{22} demonstrated strong relevance, with importance scores of 2.34 and 2.18, respectively. These values, though slightly lower than those for distance prediction, suggest that reflection coefficients play a substantial role in angle prediction. Frequency contributed moderately, with an importance score of 1.03, supporting the reflection coefficients in capturing angular alignment information. These findings align with previously discussed points on using transmission coefficients for gap alignment and reflection coefficients for angular alignment.

D. MODEL DEVELOPMENT

The development of machine learning models in this study focused on three advanced neural network architectures: MLP, CNN, and LSTM. Each model was carefully designed and optimized to capture the unique patterns and dependencies within the S-parameter dataset, enabling accurate predictions of both antenna distance and angular alignment.

1) MULTILAYER PERCEPTRON (MLP)

The MLP model was designed as a feedforward neural network with a deep architecture tailored to the dataset's high-dimensional and nonlinear characteristics. For distance prediction, the MLP architecture included six hidden layers with decreasing numbers of neurons (500, 250, 160, 100, 90, and 50), while for angle prediction, the architecture used four hidden layers (300, 150, 100, and 50). The primary operation in the MLP is the weighted sum of inputs followed by an

activation function:

$$a^{(l)} = \sigma(W^{(l)} \cdot a^{(l-1)} + b^{(l)}), \tag{2}$$

where $a^{(l)}$ is the activation in layer l, $W^{(l)}$ and $b^{(l)}$ are the weights and biases for layer l, and σ is the activation function (ReLU in this study). The MLP also uses softmax activation in the output layer for multi-class classification:

$$y_k = \frac{e^{z_k}}{\sum_{j=1}^{K} e^{z_j}}, \tag{3}$$

where y_k is the probability of class k, and z_k is the input to the softmax function for class k. The MLP was optimized using Stochastic Gradient Descent (SGD) with adaptive learning rates and Nesterov momentum, ensuring efficient convergence.

2) CONVOLUTIONAL NEURAL NETWORK (CNN)

The CNN model was developed to extract spatial patterns from the S-parameter data, which was pre-processed to include smoothed and normalized features. The architecture consisted of two convolutional layers with 128 and 64 filters, respectively, using a kernel size of 1 to adapt to the single-timestep input. These layers were followed by a flattening operation and dense layers to consolidate feature representations. The primary operation in the CNN is the convolution, defined mathematically as:

$$z_{i,j,k} = \sum_{m=1}^{M} \sum_{n=1}^{N} \left(x_{i+m,j+n} \cdot w_{m,n,k} + b_k \right), \tag{4}$$

where $z_{i,j,k}$ is the output of the convolution operation at position (i, j) for filter k, x is the input feature map, w represents the filter weights, b_k is the bias term for the k-th filter, and $M \times N$ is the filter size.

The CNN applied ReLU activation to introduce non-linearity, followed by max-pooling to reduce the spatial dimensions while preserving the most salient features. The final dense layers and softmax activation facilitated multi-class classification for both distance and angle prediction tasks.

The CNN demonstrated strong performance in predicting both distance and angle. For distance prediction, the model classified data into four categories (0 mm, 2 mm, 13 mm, and 150 mm), achieving high accuracy and reliable performance across all classes. For angle prediction, the model categorized angles into thirteen classes (0°, 30°, …, 360°) and effectively captured the cyclical nature of the data, aided by pre-processed angular features. The CNN's ability to efficiently learn spatial features made it particularly suitable for handling the S-parameter dataset's high-dimensional characteristics.

3) LONG SHORT-TERM MEMORY NETWORK (LSTM)

The LSTM model capitalized on its recurrent architecture to capture temporal dependencies within the S-parameter data. Although the dataset did not inherently have sequential time-series data, the LSTM effectively learned relationships between features within a single timestep. The model consisted of multiple LSTM layers with decreasing units (256, 128, and 64) to progressively distill information, followed by a dense output layer with softmax activation. The core operations of the LSTM are as follows:

$$f_t = \sigma(W_f \cdot [h_{t-1}, x_t] + b_f), \tag{5}$$
$$i_t = \sigma(W_i \cdot [h_{t-1}, x_t] + b_i), \tag{6}$$
$$\tilde{C}_t = \tanh(W_C \cdot [h_{t-1}, x_t] + b_C), \tag{7}$$
$$C_t = f_t \cdot C_{t-1} + i_t \cdot \tilde{C}_t, \tag{8}$$
$$o_t = \sigma(W_o \cdot [h_{t-1}, x_t] + b_o), \tag{9}$$
$$h_t = o_t \cdot \tanh(C_t), \tag{10}$$

where f_t, i_t, o_t represent the forget, input, and output gates, respectively; C_t is the cell state, h_t is the hidden state, and σ is the sigmoid activation function. These equations describe how the LSTM processes and retains relevant information while discarding irrelevant details, enabling it to model complex interdependencies within the S-parameter dataset effectively.

The LSTM model excelled in both distance and angle prediction tasks, demonstrating a robust capacity to model complex relationships within the data. Its ability to retain meaningful dependencies was particularly advantageous for distinguishing subtle patterns that correlate with specific distance and angle categories. By leveraging the inherent structure of the S-parameters, the LSTM provided reliable predictions with high accuracy.

4) EVALUATION METRICS

The performance of the CNN, LSTM, and MLP models was assessed using a comprehensive set of metrics, including accuracy, precision, recall, F1-score, and classification reports. Accuracy provided a high-level overview of each model's effectiveness, measuring the proportion of correct predictions across all classes. However, to gain deeper insights into the models' strengths and weaknesses, additional metrics such as precision and recall were calculated for each class.

Precision focused on the correctness of positive predictions, offering insights into the models' reliability in avoiding false positives. Recall, on the other hand, measured the models' ability to identify all relevant instances, capturing their effectiveness in avoiding false negatives. The F1-score, calculated as the harmonic mean of precision and recall, provided a balanced evaluation, particularly valuable in scenarios with class imbalance, such as the uneven distribution of distance or angle categories.

The classification reports included metrics for each class, allowing for a detailed breakdown of the models' performance across the four distance categories (0 mm, 2 mm, 13 mm, and 150 mm) and thirteen angular classes (0°, 30°, …, 360°). This granular analysis highlighted the strengths of the CNN and LSTM models in handling high-dimensional

and cyclical data, respectively. The MLP model, while performing competitively, offered a benchmark against which the more complex architectures demonstrated their advanced capabilities.

The evaluation emphasized the models' ability to generalize effectively, as evidenced by their performance on the held-out testing set. Together, these metrics provided a rigorous framework for assessing model performance, ensuring the reliability and validity of predictions in the context of RF engineering challenges.

IV. RESULTS AND DISCUSSION

The evaluation of machine learning models to predict the mechanical alignment of two identical antennas, quantified by both the distance and angle based on S-parameter measurements, yielded insightful outcomes. Three models—MLP, CNN, and LSTM—were rigorously assessed for their ability to classify distances and angles. The detailed classification results for distances and angles are presented in Tables 3 and 4, respectively, with corresponding confusion matrices visualized in Figures 4 to 9.

The performance of the models in classifying antenna distances (0 mm, 2 mm, 13 mm, and 150 mm) was highly competitive, as demonstrated in Table 3. The MLP and LSTM models both achieved an accuracy of 97%, while the CNN model performed slightly lower with an accuracy of 95%. These high accuracies highlight the models' capabilities in handling the discrete nature of distance classification.

The MLP model demonstrated balanced performance across all distance categories, achieving a precision, recall, and F1-score of 0.95 or higher for all classes. The confusion matrix in Figure 4 illustrates minimal misclassification, with the majority of predictions aligning perfectly with their true labels. This robustness emphasizes the MLP's ability to model the relationships between S-parameter measurements and antenna distances effectively.

In comparison, the CNN model achieved high precision and recall for most distance categories but showed slight misclassification between the closely spaced categories (0 mm and 2 mm), as evident in Figure 6. Despite these minor misclassifications, the CNN's ability to accurately distinguish larger distances, such as 13 mm and 150 mm, was near perfect.

On the other hand, the LSTM model excelled in distinguishing all four distance categories, with precision, recall, and F1-scores of 0.94 or higher for all classes, as shown in Figure 8. Its recurrent architecture proved particularly effective in capturing interdependencies within the S-parameter dataset, ensuring reliable predictions even for closely spaced categories. These results confirm that all three models are well-suited for distance prediction tasks, with the MLP and LSTM models demonstrating slightly better performance than the CNN.

Angle prediction posed a greater challenge due to the higher number of classes (13 angular categories from 0° to 360°) and the cyclical nature of the data. Nevertheless, the

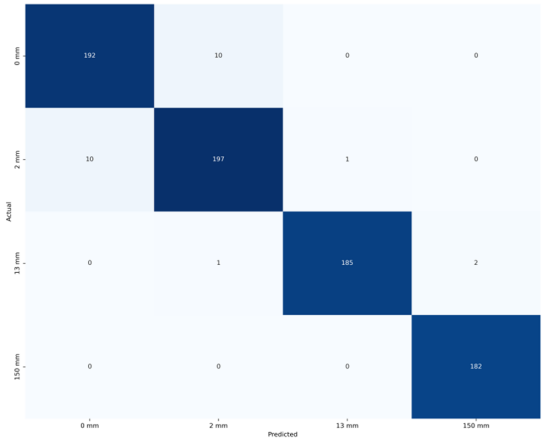

FIGURE 4. Predicted vs. Actual distances (Random forest model).

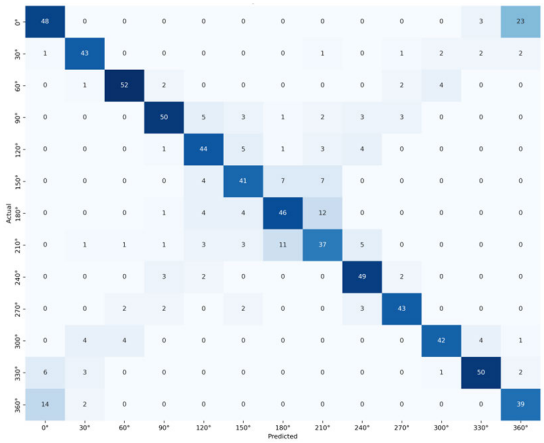

FIGURE 5. Predicted vs. Actual distances (Decision tree model).

models performed competitively, with the CNN achieving the highest accuracy of 86%, followed by the LSTM (79%) and the MLP (75%), as summarized in Table 4.

The MLP model demonstrated robust performance across several angular categories, particularly for angles like 60° and 90°, where precision and recall exceeded 0.85. However, the confusion matrix in Figure 5 reveals occasional misclassifications at the boundary angles (0° and 360°), reflecting the inherent challenges of cyclical data.

The CNN model outperformed the other architectures in angle prediction, achieving an accuracy of 86%. Its confusion matrix, presented in Figure 7, highlights its strength in distinguishing angular categories, with high precision and recall across most classes. The CNN's ability to leverage spatial patterns from the S-parameter data contributed significantly to its superior performance.

While the LSTM model achieved slightly lower accuracy compared to the CNN, it performed well in mid-range angular categories such as 120° and 180° (Figure 9). Its recurrent architecture was effective in capturing patterns within the data but struggled with boundary angles, similar to the MLP.

TABLE 3. Classification report for distance prediction models.

Distance (mm)	MLP Model				CNN Model				LSTM Model			
	Precision	Recall	F1-Score	Support	Precision	Recall	F1-Score	Support	Precision	Recall	F1-Score	Support
0	0.95	0.95	0.95	202	0.96	0.84	0.90	202	0.92	0.98	0.94	202
2	0.95	0.95	0.95	208	0.86	0.97	0.91	208	0.97	0.91	0.94	208
13	0.99	0.98	0.99	188	1.00	0.99	0.99	188	1.00	0.99	1.00	188
150	0.99	1.00	0.99	182	1.00	1.00	1.00	182	1.00	1.00	1.00	182
Accuracy			0.97				0.95				0.97	
Macro Avg.	0.97	0.97	0.97	780	0.95	0.95	0.95	780	0.97	0.97	0.97	780
Weighted Avg.	0.97	0.97	0.97	780	0.95	0.95	0.95	780	0.97	0.97	0.97	780

TABLE 4. Classification report for angle prediction models.

Angle (°)	MLP Model				CNN Model				LSTM Model			
	Precision	Recall	F1-Score	Support	Precision	Recall	F1-Score	Support	Precision	Recall	F1-Score	Support
0	0.70	0.65	0.67	74	0.85	0.78	0.82	74	0.62	0.78	0.69	74
30	0.80	0.83	0.81	52	0.89	0.98	0.94	52	0.96	0.83	0.89	52
60	0.88	0.85	0.87	61	0.95	0.93	0.94	61	0.95	0.85	0.90	61
90	0.83	0.75	0.79	67	0.85	0.96	0.90	67	0.89	0.82	0.85	67
120	0.71	0.76	0.73	58	0.90	0.90	0.90	58	0.85	0.81	0.83	58
150	0.71	0.69	0.70	59	0.80	0.73	0.76	59	0.70	0.56	0.62	59
180	0.70	0.69	0.69	67	0.85	0.84	0.84	67	0.74	0.81	0.77	67
210	0.60	0.60	0.60	62	0.81	0.82	0.82	62	0.73	0.82	0.77	62
240	0.77	0.88	0.82	56	0.83	0.80	0.82	56	0.75	0.84	0.79	56
270	0.84	0.83	0.83	52	0.98	0.98	0.98	52	0.86	0.92	0.89	52
300	0.86	0.76	0.81	55	0.98	0.96	0.97	55	0.93	0.96	0.95	55
330	0.85	0.81	0.83	62	0.73	0.82	0.77	62	0.77	0.71	0.74	62
360	0.58	0.71	0.64	55	0.73	0.65	0.69	55	0.70	0.58	0.63	55
Accuracy			0.75				0.86				0.79	
Macro Avg.	0.75	0.75	0.75	780	0.86	0.86	0.86	780	0.80	0.79	0.79	780
Weighted Avg.	0.75	0.75	0.75	780	0.86	0.86	0.86	780	0.80	0.79	0.79	780

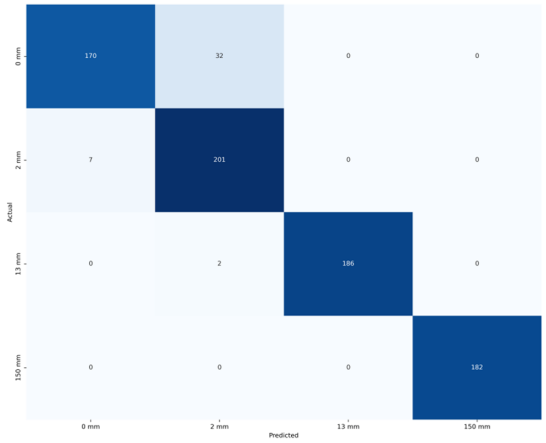

FIGURE 6. Predicted vs. Actual distances (MLP model).

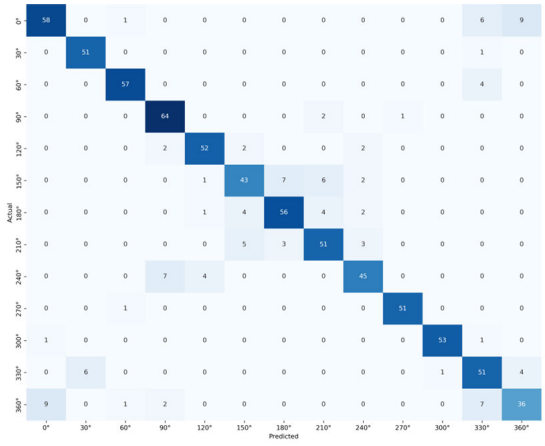

FIGURE 7. Predicted vs. Actual angles (MLP model).

The comparative analysis of the models reveals distinct strengths and limitations. For distance prediction, the MLP and LSTM models demonstrated exceptional performance, with the LSTM model excelling in scenarios requiring precise differentiation between closely spaced categories. For angle prediction, the CNN model stood out due to its ability to handle high-dimensional and cyclical data, achieving the highest accuracy among the three models. The confusion matrices provide valuable insights into the models' prediction patterns, highlighting areas of strength, such as accurate

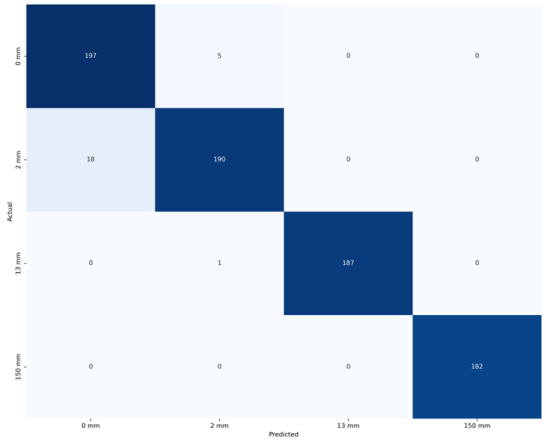

FIGURE 8. Predicted vs. Actual angles (Random forest model).

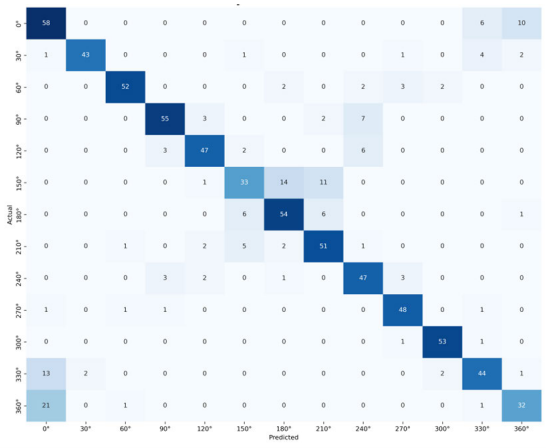

FIGURE 9. Predicted vs. Actual angles (Decision tree model).

classification of 13 mm and 150 mm distances, and areas for improvement, such as boundary angle misclassification.

The findings from this study emphasize the importance of selecting model architectures tailored to the specific characteristics of the prediction task. Compared to traditional alignment techniques, such as optical and acoustic methods, the machine-learning-based approach demonstrated in this study offers a streamlined solution with high predictive accuracy. For instance, previous studies involving imaging-based alignment methods reported complexities in setup and calibration [10], whereas our approach requires only standard S-parameter measurements, reducing implementation costs. Optical transmission methods [11] and non-contact acoustic methods [12] have also been explored, but these often require specialized equipment or feedback systems, increasing complexity and limiting scalability. In contrast, our results demonstrate the effectiveness of machine learning in achieving precise antenna alignment without extensive hardware.

V. CONCLUSION

This study explored the application of machine learning models—MLP, CNN, and LSTM—in addressing a fundamental challenge in RF engineering: accurate antenna alignment through distance and angle predictions based on S-parameter measurements. By leveraging the predictive power of these neural network architectures, we sought to improve the precision of mechanical alignment, a critical factor for ensuring optimal communication performance. The results demonstrate the diverse strengths and limitations of each model, offering valuable insights into their applicability for RF engineering tasks.

In distance prediction, the MLP and LSTM models emerged as the leading performers, both achieving an impressive accuracy of 97%. The LSTM model excelled in capturing interdependencies within the dataset, enabling it to reliably distinguish between closely spaced categories, such as 0 mm and 2 mm. Meanwhile, the MLP model demonstrated balanced performance across all distance categories, with precision, recall, and F1-scores exceeding 0.95 for all classes. The CNN model, although slightly lower in accuracy at 95%, showed its strength in predicting larger distances, such as 13 mm and 150 mm, with near-perfect precision and recall. Together, these results underscore the reliability and robustness of these models in handling the discrete nature of distance classification tasks.

Angle prediction posed a greater challenge due to the higher number of classes and the cyclical nature of the data. The CNN model achieved the highest accuracy of 86%, outperforming the LSTM and MLP models. The CNN's ability to extract spatial patterns from the high-dimensional S-parameter data allowed it to excel in most angular categories. The LSTM model demonstrated strong performance in mid-range angular categories, while struggling with boundary angles. Although the MLP model achieved the lowest accuracy among the three models, it performed competitively in several categories, demonstrating its capacity to handle complex, nonlinear relationships in the data. The findings highlight the importance of selecting model architectures tailored to the unique characteristics of the prediction tasks.

The results of this study emphasize the potential of machine learning in addressing antenna alignment challenges. The CNN model's superior performance in angle prediction, coupled with the MLP and LSTM models' exceptional capabilities in distance prediction, demonstrates the versatility of these neural network architectures. Also, the confusion matrices provide valuable insights into areas where model performance can be further improved, such as reducing misclassifications at boundary angles.

While the study offers significant contributions to RF engineering, several limitations must be acknowledged. The experimental setup involved specific antenna types and controlled indoor conditions, which may not fully generalize to other configurations or variable environments such as

outdoor deployments or mobile systems. Additionally, the dataset was collected using a single dielectric material, which could limit the models' adaptability to diverse material and structural variations encountered in real-world scenarios. These constraints highlight opportunities for future research to improve the robustness and generalizability of the proposed models.

Future directions could involve expanding the dataset to encompass a wider variety of antenna designs, materials, and environmental conditions. Investigating more advanced learning architectures—such as hybrid CNN-LSTM models—and exploring real-time adaptive algorithms would be valuable for deployment in dynamic RF environments. Transfer learning may also accelerate model convergence and performance in low-data or rapidly changing conditions, thus broadening applicability across RF domains.

Moreover, deploying these models in practical systems—such as IoT nodes, wireless sensor networks, and 5G base stations—offers exciting possibilities. Automated systems for continuous antenna alignment, powered by machine learning, could enhance network reliability, reduce calibration effort, and support intelligent infrastructure. Evaluating model behavior in time-varying conditions and integrating these algorithms with modern RF technologies, including phased arrays and software-defined radios, could pave the way for scalable, self-correcting wireless communication systems.

REFERENCES

[1] S. De Silva, L. Belostotski, and M. Okoniewski, "Modeling and measuring of antenna array s-parameters and radiation efficiency," in *Proc. IEEE Int. Symp. Antennas Propag. USNC/URSI Nat. Radio Sci. Meeting*, Jul. 2017, pp. 2293–2294, doi: 10.1109/APUSNCURSINRSM.2017.8073189.

[2] J. Thaysen and K. B. Jakobsen, "Envelope correlation in (N, N) MIMO antenna array from scattering parameters," *Microw. Opt. Technol. Lett.*, vol. 48, no. 5, pp. 832–834, May 2006.

[3] N. Ambasana, G. Anand, D. Gope, and B. Mutnury, "S-parameter and frequency identification method for ANN-based eye-height/width prediction," *IEEE Trans. Compon., Packag., Manuf. Technol.*, vol. 7, no. 5, pp. 698–709, May 2017, doi: 10.1109/TCPMT.2017.2661065.

[4] M. A. Bataineh, M. M. Umar, A. Moin, M. I. Hussein, and M. A. Ahmad, "Classification and prediction of communication cables length based on S-parameters using a machine-learning method," *IEEE Access*, vol. 11, pp. 108041–108049, 2023, doi: 10.1109/ACCESS.2023.3320581.

[5] X. Ling and R. Li, "A novel dual-band MIMO antenna array with low mutual coupling for portable wireless devices," *IEEE Antennas Wireless Propag. Lett.*, vol. 10, pp. 1039–1042, 2011, doi: 10.1109/LAWP.2011.2169035.

[6] Z. Qiu, Y. Lu, and Z. Qiu, "Review of ultrasonic ranging methods and their current challenges," *Micromachines*, vol. 13, no. 4, p. 520, Mar. 2022, doi: 10.3390/mi13040520.

[7] S. Adarsh, S. M. Kaleemuddin, D. Bose, and K. I. Ramachandran, "Performance comparison of infrared and ultrasonic sensors for obstacles of different materials in vehicle/ robot navigation applications," *IOP Conf. Ser. Mater. Sci. Eng.*, vol. 149, Sep. 2016, Art. no. 012141, doi: 10.1088/1757-899x/149/1/012141.

[8] T. Oka, H. Nakajima, M. Tsugai, U. Hollenbach, U. Wallrabe, and J. Mohr, "Development of a micro-optical distance sensor," *Sens. Actuators A, Phys.*, vol. 102, no. 3, pp. 261–267, Jan. 2003, doi: 10.1016/S0924-4247(02)00395-3.

[9] Y. S. Suh, "Laser sensors for displacement, distance and position," *Sensors*, vol. 19, no. 8, p. 1924, Apr. 2019, doi: 10.3390/s19081924.

[10] C. Zhang, J. Pu, and X. Niu, "An autonomous robotic alignment strategy based on visual guidance," *IOP Conf. Ser. Mater. Sci. Eng.*, vol. 612, no. 3, Oct. 2019, Art. no. 32123, doi: 10.1088/1757-899X/612/3/032123.

[11] M. Abdolahi, A. A. Adawi, H. Jiang, and B. Kaminska, "Light-blocking optical alignment rulers for guiding layer-by-layer integration," *J. Lightw. Technol.*, vol. 37, no. 14, pp. 3655–3664, Jul. 14, 2019, doi: 10.1109/JLT.2019.2918762.

[12] T. Furumoto, K. Hasegawa, Y. Makino, and H. Shinoda, "Three-dimensional manipulation of a spherical object using ultrasound plane waves," *IEEE Robot. Autom. Lett.*, vol. 4, no. 1, pp. 81–88, Jan. 2019, doi: 10.1109/LRA.2018.2880330.

[13] T. O'Shea and J. Hoydis, "An introduction to deep learning for the physical layer," *IEEE Trans. Cognit. Commun. Netw.*, vol. 3, no. 4, pp. 563–575, Dec. 2017, doi: 10.1109/TCCN.2017.2758370.

[14] S. Rajendran, W. Meert, D. Giustiniano, V. Lenders, and S. Pollin, "Deep learning models for wireless signal classification with distributed low-cost spectrum sensors," *IEEE Trans. Cognit. Commun. Netw.*, vol. 4, no. 3, pp. 433–445, Sep. 2018, doi: 10.1109/TCCN.2018.2835460.

[15] F. Hu, B. Chen, and K. Zhu, "Full spectrum sharing in cognitive radio networks toward 5G: A survey," *IEEE Access*, vol. 6, pp. 15754–15776, 2018, doi: 10.1109/ACCESS.2018.2802450.

[16] B. Tasci and Y. Erol, "An embedded communication system solution for operation in the presence of RF noise and interference," *Microwave J.*, vol. 66, no. 12, 2023.

[17] I. Ahmad, S. Shahabuddin, H. Malik, E. Harjula, T. Leppänen, L. Lovén, A. Anttonen, A. H. Sodhro, M. M. Alam, M. Juntti, A. Ylä-Jääski, T. Sauter, A. Gurtov, M. Ylianttila, and J. Riekki, "Machine learning meets communication networks: Current trends and future challenges," *IEEE Access*, vol. 8, pp. 223418–223460, 2020, doi: 10.1109/ACCESS.2020.3041765.

[18] J. Zhang and K. B. Letaief, "Mobile edge intelligence and computing for the Internet of Vehicles," in *Proc. IEEE*, vol. 108, Oct. 2019, pp. 246–261, doi: 10.1109/JPROC.2019.2947490.

[19] N. Sarker, P. Podder, M. R. H. Mondal, S. S. Shafin, and J. Kamruzzaman, "Applications of machine learning and deep learning in antenna design, optimization, and selection: A review," *IEEE Access*, vol. 11, pp. 103890–103915, 2023, doi: 10.1109/ACCESS.2023.3317371.

[20] M. Geiger and C. Waldschmidt, "160-GHz radar proximity sensor with distributed and flexible antennas for collaborative robots," *IEEE Access*, vol. 7, pp. 14977–14984, 2019, doi: 10.1109/ACCESS.2019.2891909.

[21] S. Capdevila, L. Jofre, J.-C. Bolomey, and J. Romeu, "RFID multiprobe impedance-based sensors," *IEEE Trans. Instrum. Meas.*, vol. 59, no. 12, pp. 3093–3101, Dec. 2010, doi: 10.1109/TIM.2010.2063053.

[22] G. Gupta, B. P. Singh, A. Bal, D. Kedia, and A. R. Harish, "Orientation detection using passive UHF RFID technology [education column]," *IEEE Antennas Propag. Mag.*, vol. 56, no. 6, pp. 221–237, Dec. 2014, doi: 10.1109/MAP.2014.7011063.

[23] D. M. Pozar, *Microwave Engineering*, 4th ed., Hoboken, NJ, USA: Wiley, 2011.

[24] R. Sanmugasundaram, S. Natarajan, and R. Rajkumar, "A compact MIMO antenna with electromagnetic bandgap structure for isolation enhancement," *Prog. Electromagn. Res. C*, vol. 107, pp. 233–244, 2021, doi: 10.2528/pierc20111306.

[25] T. C. Chau, B. A. Welt, and W. R. Eisentadt, "Analysis and characterization of transponder antennae for radio frequency identification (RFID) systems," *Packag. Technol. Sci.*, vol. 19, no. 1, pp. 33–44, Jan. 2006, doi: 10.1002/pts.709.

[26] P. Gas, "Optimization of multi-slot coaxial antennas for microwave thermotherapy based on the s 11 -parameter analysis," *Biocybern. Biomed. Eng.*, vol. 37, no. 1, pp. 78–93, 2017, doi: 10.1016/j.bbe.2016.10.001.

[27] C. A. Balanis, *Antenna Theory: Analysis and Design*, 4th ed., Hoboken, NJ, USA: Wiley, 2016.

[28] H. G. Schantz, "Theory and practice of near-field electromagnetic ranging," in *Proc. I_{ON} Int. Tech. Meeting*, Feb. 2012, pp. 978–1013.

[29] *R&S ZVL Vector Network Analyzer*, Rohde & Schwarz, Munich, Germany, 2023.

MOHAMMAD AL BATAINEH received the B.S. degree (Hons.) in telecommunications engineering from Yarmouk University, Jordan, in 2003, and the M.S. and Ph.D. degrees in electrical engineering from Illinois Institute of Technology (IIT), USA, in 2006 and 2010, respectively. Subsequent to his academic pursuits, he held noteworthy positions at institutions, including Yarmouk University, where he was promoted as an Associate Professor, in 2018, and roles with Argonne National Laboratories and MicroSun Technologies. In August 2020, he joined United Arab Emirates University (UAEU), as an Assistant Professor. His research interests include the application of communications, coding theory, and information theory to the interpretation and understanding of information flow in biological systems, particularly gene expression. His additional research avenues encompass machine learning, network information theory, and optimization.

DANA I. ABU ABDOUN received the B.Sc. and M.Sc. degrees in industrial engineering and engineering management from the University of Sharjah, United Arab Emirates, in 2018 and 2022, respectively. She is currently a Research Assistant at the College of Engineering (COE), specifically in the Department of Electrical and Communications Engineering, United Arab Emirates University. Her research interests include data mining, machine learning, additive manufacturing, and supply chain management.

MAHMOUD AL AHMAD (Senior Member, IEEE) received the B.Sc. degree in electrical engineering from Birzeit University, Ramallah, Birzeit, in 1999, and the M.Sc. and Ph.D. degrees in microwave engineering from Technische Universität München, Munich, Germany, in 2002 and 2006, respectively. He is currently a Faculty Member with the Department of Electrical Engineering, United Arab Emirates University. He has over ten years of electronic materials and device fabrication research experience in academia, national laboratories, and industry. He has managed several research projects and teams with annual budgets of up to U.S. $1 million. He has also conducted research in energy harvesting technologies and frequency agile circuits with Siemens AG/CNRS and with the King Abdullah University of Science and Technology (KAUST), and has authored or co-authored more than 20 journal and 35 conference papers in this domain, with more under review. He is a Principal (Lead) Author of around 55 published papers in journals and international conferences and has delivered over 40 presentations at international conferences, several of which have been invited talks. His research interests include the design and fabrication of self-powered, low-power nano-based electronic devices and systems, and applied electromagnetics for biomedical applications.